

The Influence of Friction Stir Welding and Process Parameters on the Static and Dynamic Mechanical Properties of 2024-T3 Aluminum Alloy Weldments

Dr. Shaker S. Hassan

Machines & Equipments Engineering Department, University of Technology/ Baghdad
Email: Shaker_Sakran1952_1@yahoo.com

Dr. Moneer H. Tolephih

Technical College Baghdad, Foundation of Technical Education/ Baghdad
Email: monerht@yahoo.com

Nameer A. Hamoody

Technical College Baghdad, Foundation of Technical Education/ Baghdad
Email: alsaadinameer@yahoo.com

Received on: 27 /4 /2011 & Accepted on: 1 /12/2011

ABSTRACT

The present work is aimed to study the friction stir welding and process for the aluminum alloy 2024-T3, a threaded pin with a diameter of 6 mm and a concaved shoulder of 18 mm welding tool was used. The single pass friction stir welding (FSW) process was performed with clockwise tool rotation at different speeds and variable feeding speeds. The specimens were tested to determine the best ultimate tensile strength (σ_{ult}) and compared with the as received metal. In addition to friction stir welding (FSW), another phase of welding named friction stir process (FSP) was used. The best condition out of the FSW variables was selected in order to examine the double pass welding processes. It was found that the best result is in forward welding travel and counterclockwise tool rotation. The maximum tensile strength achieved at friction stir welding process was 72% of the base metal and didn't improve in the FSP process. On the other hand, the fatigue endurance limit was improved for FS weld ment when followed by FSP, where the reduction in fatigue endurance limit for FSW specimen was 36% while for FSP specimen was 15% of the base metal.

Keywords: Friction stir welding, Double pass, Aluminum alloy

تأثير متغيرات لحام و عملية الخلط الاحتكاكي على الخواص الميكانيكية السكونية والديناميكية لمعلومات سبيكة الألمنيوم T3 – 2024

الخلاصة

يهدف البحث الحالي الى دراسة لحام وعملية الخلط الاحتكاكي لسبيكة الألمنيوم 2024-T3 حيث تم استخدام عدة اللحام المتكونة من الجزء المتغلغل بقطر 6 ملم ويكون مسنن ذو كتف مقعر بقطر 18 ملم. تم إجراء لحام الخلط الاحتكاكي بشوط واحد وسرع دوران مختلفة لعدة اللحام مع عقارب الساعة وكذلك سرع متغيرة للتغذية. تم فحص النماذج لأختيار أقصى متانة شد مقارنة مع المعدن الأساس المستخدم. كما تم استخدام شوط ثاني يطلق عليه عملية الخلط الاحتكاكي بالإضافة الى شوط لحام

الخلط الاحتكاكي. تم اختيار افضل حالة ناتجة من متغيرات لحام الخلط الاحتكاكي لغرض اختبار عمليات اللحام بشوطين وقد بينت النتائج أن أفضل ظروف هي عند المحافظة على اتجاه التغذية و باتجاه دوران العدة معاكس لعقارب الساعة. ان اعلى متانة شد تحققت في لحام الخلط الاحتكاكي كانت 72% من المعدن الأساس ولم تتحسن في عملية الخلط الاحتكاكي. من ناحية اخرى قد تحسن حد الكلال لمحومة الخلط الاحتكاكي عندما تبعت بعملية الخلط الاحتكاكي حيث كان النقصان في حد الكلال لعينة لحام الخلط الاحتكاكي 36% بينما كان حد الكلال لعينة عملية الخلط الاحتكاكي 15% من المعدن الأساس.

Notations

AS	Advanced side
c.w.	Clock-wise
c.c.w.	Counterclockwise
FSP	Friction Stir Processing
FSW	Friction Stir Welding
N_f	Number of Cycles to Failure(Cycles)
R	Stress Ratio
RS	Retreating Side
σ_f	Fatigue strength(MPa)
$\sigma_{E.L.}$	Fatigue Endurance Limit(MPa)
σ_{Ult}	Ultimate Tensile Strength(MPa)

INTRODUCTION AND LITERATURE REVIEW

Friction stir welding (FSW) is a relatively new solid state welding process invented at The Welding Institute (Cambridge, UK) in 1991. [1]. This technique is well suited for welding heat treatable aluminum alloys, especially for the 2xxx series, which is usually considered as unweldable by conventional welding processes [2]. This joining process has gathered a great amount of interest in a variety of applications in aerospace, automotive, marine, railway, and construction industries [3, 4].

The maximum temperature measured during friction stir welding of aluminum alloys falls between 0.7 and 0.9 of melting point [5]. That means that the metal reaches a temperature enough to soften but not melt, so that the welding defects and large distortion commonly associated with the fusion welding are minimized or avoided [6].

Figure 1 illustrates the schematic diagram of FSW as applied to a butt joint of two plates. The workpiece to be welded is supported by a backing plate and clamped rigidly by an anvil to prevent the lateral movement during the welding [7]. A rotating, non-consumable tool consisting of a small-diameter pin extending down from a larger diameter shoulder is plunged into the joint line and is then traversed along that line [8]. The shoulder is slightly concave. The concavity is designed to provide a reservoir of material above the original crown surface of the weld, facilitates transport of material around the tool, and reduces plate thinning in the weld zone [9]. The advancing side (AS) is the side where the velocity vectors of the tool rotation and

traverse direction are similar and the side where the velocity vectors are opposite is referred as the retreating side (RS)[10].

In most of the published researches that utilizes friction stir welding, single pass Welding process was used to fabricate the joints [1-5, 8, 10]. Only few researches concerned with double pass welding process. H. Jin et al [11] focused on the diffusion and microstructure of the metals at the interface of Iron – Nickel double pass butt welded joints, while for L. Dubourg et al [12], a partial overlap of the advancing sides of the welding passes was used as a double pass welding process to fabricate lap joints of AA7075-T6 stringers on AA2024-T3 skin.

The aim of the current work is to study the parameters affecting the friction stir welding for AA2024-T3 sheets of metal and the effect on some mechanical properties. In addition to that, the work is concerned with the influence of an additional pass denoted as friction stir process (FSP), i.e., (double pass welding process) on some of mechanical properties.

EXPERIMENTAL WORK

A rolled section of 5 mm thick sheet of a heat treatable aluminum alloy n AA2024-T3, was used in the as received condition as the base material in this investigation. The chemical composition and mechanical properties listed in Table 1 and 2. The sheet was cut and machined into rectangular welding samples of 200mm long by 100mm wide. Every two samples were secured into a carbon steel backing plate using specially designed mechanical clamps to avoid separation or lateral movement from the joint line during the welding process. The welding samples were then longitudinally butt-welded perpendicular to sheet rolling direction using a vertical type milling machine. During the welding cycles, the tool was rotating in the clock-wise direction and was tilting 2 degrees with respect to a vertical axis. The downward pressure of the tool was kept constant throughout the experiments by keeping the plunging depth of the tool shoulder fixed.

Four selected rotational speeds (370, 475, 650, and 820) rpm were used in the welding process with welding travel speeds of (24, 42, and 74) mm/min. The best condition for the above test variables base on tensile test was chosen to study the mechanical properties as well as to run FSP. Four conditions were carried out with the two directions of tool rotation and welding orientation.

The friction stir welding tool was fabricated from tool steel (X12M) with a hardness of 58 HRC. The tool had an 18mm diameter concaved shoulder (8°), while the tool pin is of 6mm diameter with a right hand threads of (1) mm pitch and have a round bottom. The overall height of the pin is (4.7) mm, making it slightly shorter than the sheet thickness Fig (2).

Tensile testing was carried out on samples cut perpendicular to the welding direction to determine the tensile properties of the welded joints for both single and double pass of welding, where the size of the tensile specimens was carried according to ASTM B557M [13]. Tensile properties of each joint were evaluated at room temperature and constant crosshead speed of 5mm/min using the computerized (Zwick/Roell 100 KN) Universal testing machine at Technical College Baghdad. All tensile tests were carried out at a constant crosshead speed of 5 mm/min.

Microhardness measurements were taken 2 mm below the top surface of the specimens, perpendicular to the welding direction. Microhardness (HV0.05) testing of the welded joints was conducted using a Zwick/Roell microhardness testing machine at Central Organization for Standardization and Quality Control with a load of (50 g) and loading within (15 sec) according to ASTM-E384 [13].

Bending fatigue tests were carried out through fatigue machine (Avery Dension Ltd Fatigue Testing Machine type 7305) at Central Organization for Standardization and Quality Control, with stress cycles 1420 rpm. The tests were carried out at room temperature. The shape and dimensions of the fatigue specimens prepared according to DIN 50113 are shown in figure (3). Completely reversed loads of an opposite sign were applied at stress ratio $R=-1$. Eight specimens were tested for each kind of joint and base metal. The range of maximum stress was varied from 384 MPa to 196 MPa for the base material as unwelded. In a different way, the range for the joints with a single pass was from 274 MPa to 140 MPa, and for the joints using a double pass welding process, the range was from 265 MPa to 136 MPa. The number of cycles to fracture was recorded or the test was stopped at 10^7 cycles without break down of joint.

RESULTS AND DISCUSSION

Tensile Test Results

Two stages of tensile tests were carried on, the first for welding trials with a single pass welding process and the second with a double pass welding. Table 3 lists the first stage tensile test results of friction stir welded joint. The table shows the variation of tensile properties according to test variables. The heat input which is mainly affecting the welding parameters plays an important role in the tensile properties. In addition to heat input, the tensile properties are also dependent on the welding defects. The maximum ultimate tensile strength which gives the best welding efficiency of (72 %) occurred in a combination of 370 rpm tool rotational speed and 24 mm/min welding travel speed.

Table 4 shows the tensile properties of the joints welded using double pass process at different welding orientation and tool rotation direction, the tool rotational speed and travel speed are maintained constant and taken from the best welding parameters for the single pass process. This table indicates that the best ultimate tensile strength of (332 MPa) and elongation of (4.84%) with a weld efficiency of (69%) can be achieved when using a double pass with a welding travel in the same direction and a clock wise tool rotation for the first pass and a counter clock wise tool rotation for the second pass. So, the double pass process increases the ductility of the welded joint with a little decrease in the ultimate tensile stress (about 3%). The higher elongation occurred in the samples indicates that the metal was homogeneously stirred throughout the welded joint. For those samples with limited elongation, a separating area between the stir zone and the base metal were found in the fracture surface of the welded joint, as shown in figure (4). In other words, the heat that is generated due to stir, will not be sufficient to produce the welding process, as a result, defects will appear in form of separation cracks at the welding zones. On the other hand, the feeding speed (welding travel speed) also affect the strength of the welded joint. It

was found that when the welding travel speed is too fast, a wormhole defect will appear which is caused by insufficient time for stir metal in front of the tool pin to replace the cavity created behind the pin as it moves forward along the welding line. The effect of these defects will appear as a sudden fracture in specimens, i.e., reduction in elongation, fig. (5).

Most of the specimens fractured in the tensile test through the HAZ of the advanced side, fig (6), and that conforms to G. R. Babu [4]. This is matched by S. R. Ren et al. [14] who clarifies that the fracture usually occurs in the HAZ due to the significant coarsening of the strengthening precipitates.

Microhardness Results

According to the results of the tensile test, the best condition for the selective variable in the process is 370 rpm rotational speed, while the travel speed is 24 mm/min to study the microhardness distribution 2mm below the top surface cross the welded joint, i.e., perpendicular to the welding direction. Fig (7) shows the microhardness distribution across the FSW join for single pass and double pass.

The hardness of the base metal was recorded to be about (160 HV0.05), while the minimum hardness recorded for single pass welded sample at the HAZ was about (106 HV0.05) which accounts about 66% of the base metal, and the minimum hardness recorded for the NZ was about (114 HV0.05) which account about 71% of the base metal. The welding process affected the microhardness values by reducing them significantly, and when compared with that of the base metal, the difference should be due to the amount of heat generated in the welded zone which caused softening of the nugget, TMAZ, and HAZ due to dissolution and coarsening of the strengthening precipitates during the welding process [15]. Most of the specimens were fractured in the tensile test through the HAZ and that fracture is due to the distribution of microhardness values, in which the lowest value recorded in the HAZ, and this fact meets the conclusion of A. Barcellona et al. [16], who concluded that the local material softening which occurred in the weld area.

After the FS process the minimum hardness achieved was (92 HV0.05) at HAZ. It is clearly observed that the microhardness values were increased slightly in the nugget as compared to those of single pass due to the effect of the recrystallization of the nugget and the more fineness of the grains, while at the HAZ the microhardness decreased because of generating a high homogeneity in the grains in both sides of stir pin (i.e., the retreat and advance sides). The ratio of decreasing microhardness was (13 %) for double pass.

Fatigue Test Results

The S-N curves for the base metal, single pass (FSW), and double pass (FSW and FSP) welded joints are shown in fig (8). From the experiments when the value of bending stress decreased, the number of cycles increases where the life of the base metal sample at (384 MPa) was (132×10^3) cycle and it would be more than 10^7 cycle when the applied bending stress was (196 MPa) (without failure).

For FS welded specimens with single pass, it was found that there was a decrease in the life when compared with the base metal. This reduction in life may be caused by the grain refinement in stirred zone as well as the change in micro hardness through the weldment. This means that there will be a significant change in the residual

stresses which play an affective role in the life of the joint. For all fatigue specimens, the crack propagates observed in the nugget zone due to the presence of some defects like wormhole. However, the aluminum alloy 2024-T3 shows a low fatigue behavior at high stress amplitude, it can be considered an unexpected result because the tensile strength has shown a good performance. Therefore, it seems to be that the welding parameters have a direct impact on the fatigue behavior for high and low stresses and that matches the results of P. Cavaliere et. al.[17].

For the third group of specimens that are welded with double pass process (FSW and FSP), the results showed improvement in life when compared with single pass weldment. One of the reasons for improving the fatigue life was the tool rotation in c.c.w. and resulting in changing the position of the advance and retreat sides, i.e., it leads to make the region more homogenous and at the same time assists to redistribute the residual stresses around the nugget. On the other hand, the elongation was improved by 29% relative to the single pass, because of the additional compressive load caused by c.c.w. direction of the tool rotation in double pass welding process which helps to treat the defect. This reduction in defect may be another reason for fatigue life improvement. Most of the failures in the fatigue specimens were at the region outside the HAZ, while some of them were propagate at HAZ and the crack grew outside the HAZ towards the base metal, and the others were propagate in the base metal. These results came from the nature of the residual stresses in the region around the nugget, the results lead to compressive residual stresses, playing a role in improving the life, and it requires more experimental investigation.

The fatigue curve equations are as follows:

For base metal $\sigma_{f(MPa)} = 1724 N_f^{-0.128} \dots\dots\dots(1)$

For single pass $\sigma_{f(MPa)} = 1306 N_f^{-0.139} \dots\dots\dots(2)$

For double pass $\sigma_{f(MPa)} = 864 N_f^{-0.095} \dots\dots\dots(3)$

After substitution the value of N_f equal to 10^7 cycles in each equation, the fatigue endurance limit (σ_{EL}) values were 219 MPa for the base metal, 138 MPa for single pass, and 186 MPa for double pass. By comparing the value of fatigue endurance limit in each welding process with that of the base metal, there is about 36% reduction in fatigue endurance limit in single pass process and about 15% reduction in fatigue endurance limit in case of double pass, which gives a clear indication that there is improvement in fatigue endurance limit for double pass process compared with single pass.

CONCLUSIONS

The FSW is a process suitable to weld the aluminum alloy that is not weldable and achieves about 72% of the ultimate tensile strength of the base metal.

1. Most of the failures in stir welded tensile test specimens occurred on the advanced side.
2. The fatigue endurance limit is improved for FS weldment when followed by FSP (about 21%), where the reduction in fatigue endurance limit for FSW specimen was 36% while for FSP specimen was 15% of the base metal.
3. A FSP follows a FSW slightly affect the ultimate tensile strength (not more than 3%), which means that the stirring process will not significantly affect the grain refinement but it will apply additional compressive load on the metal during the second pass process.
4. Most of the cracks propagated in NZ according to some defect like wormhole, while in the specimen welded and followed by FSP, the crack propagated in HAZ and B.M. where the NZ is defect free.

REFERENCES

- [1] Sakthivel, T., Sengar, G. S., and Mukhopadhyay, J., "Effect of Welding Speed on Microstructure and Mechanical Properties of Friction-Stir-Welded Aluminum", *Int J Adv. Manuf. Technol.*, (2009), pp. 468–473.
- [2] Aydın, H., Bayram, A., A. Uğuz, and K. S. Akay, "Tensile Properties of Friction Stir Welded Joints of 2024 Aluminum Alloys in Different Heat-Treated-State", *Journal of Materials and Design*, 30, (2009), pp. 2211–2221.
- [3] Lim, S.K., Lee, G.G., and Sungjoon, K., "Tensile Behavior of Friction-Stir-Welded Al 6061-T651", *Metallurgical and Materials Transactions A*, Vol. (35A), (2004), pp. 2829–2835.
- [4] Babu, G.R., Murti, K.G.K., and Janardhana, G.R., "An Experimental Study on the Effect of Welding Parameters on Mechanical and Microstructural Properties of AA 6082-T6 Friction Stir Welded Butt Joints", *ARNP Journal of Engineering and Applied Sciences*, Vol. 3, No. 5, October 2008, pp. 68–74.
- [5] Attallah, M.M., Davis, C.L., and Strangwood, M., "Microstructure-Microhardness Relationships in Friction Stir Welded AA5251", *J. of Mater. Sci.*, (2007), 42, pp. 7299–7306.
- [6] Vepakomma, K.H., "Three Dimensional Thermal Modeling of Friction Stir Processing", Master Thesis, The Florida State University, Spring Semester, 2006.
- [7] Song, M., and Kovacevic, R., "Numerical and Experimental Study of the Heat Transfer Process in Friction Stir Welding", *J. of Engineering Manufacture*, Vol. 217, 2003, pp. 73–85.
- [8] Fonda, R.W., and Bingert, J.F., "Microstructural Evolution in the Heat-Affected Zone of A Friction Stir Weld", *Metallurgical and Materials Transactions A*, vol. 35, Number 15, 2004, pp. 1487–1499.
- [9] Totten, G.E., and Mackenzie, D.S., "Handbook of Aluminum", Marcel Dekker, Inc., New York, Volume 2, 2003.

[10] Kumar.K., and Kailas.S.V., “The Role of Friction Stir Welding Tool on Material Flow and Weld Formation”, Journal of Materials Science and Engineering A 485, (2008), pp. 367-374 .

[11] Jin.H., Ayer.R., Mueller.R., and Ling.S., “Metallography of dissimilar Fe-Ni Joint by Friction Stir Welding”, Proceeding of the Fifth International Offshore and Polar Engineering Conference, Seoul, Korea , 2005.

[12] Dubourg.L., Merati.A., and Jahazi.M., “Process Optimization and Mechanical Properties of Friction Stir Lap Welds of 7075-T6 Stringers on 2024-T3 Skin”, Journal of Material and Design 31,2010, Pp. 3324-3330.

[13] Annual Book of ASTM Standards, “Metal Test Methods and Analytical Procedures”, American Society for Testing and Material, Volume 03.01, Section3, 1988.

[14] Ren.S.R., Ma.Z.Y., and Chen.L.Q., “Effect of Welding Parameters on Tensile Properties and Fracture Behavior of Friction Stir Welded Al-Mg-Si Alloy”, ScriptaMaterialia 56, October 2006, pp. 69-72.

[15] Srivatsan.T.S., Vasudevan.S., and Park.L., “The Tensile Deformation and Fracture Behavior of Friction Stir Welded Aluminum Alloy 2024”, Journal of Materials Science and Engineering A 466,(2007), pp. 235-245.

[16] Barcellona.A., Buffa.G., Fratini.L., and Palmeri.D., “ On Microstructural Phenomena Occurring in Friction Stir Welding of Aluminum Alloys”, Journal of Materials Processing Technology, 177, 2006, pp. 340-343.

[17] Cavaliere.P., Campanile.G., Panella.F., and Squillace.A., “Effect of Welding Parameters on Mechanical and Microstructural Properties of AA6056 Joints Produced by Friction Stir Welded”, Journal of Materials Processing Technology 180, 2006, pp. 263-270.

Table (1) The standard and actual chemical composition of AA 2024-T3 Al alloy.

Component	Si	Fe	Cu	Mn	Mg	Cr	Zn	Ti	Ni	Pb	Sn	Al
Standard Values (ASM)Wt%	0.5 Max	0.5 Max	3.8- 4.9	0.3- 0.9	1.2- 1.8	0.10 Max	0.25 Max	0.15 Max	0.05 Max	0.05 Max	0.05 Max	Bal.
Actual Values Wt%	0.092	0.194	4.10	0.644	1.31	0.011	0.142	0.018	0.012	0.006	0.003	Bal.

Table (2) Mechanical properties of the base metal .

Yield strength(MPa)	Ultimate tensile strength(MPa)	Elongation %	Hardness(HV0.05)
350	480	19.87	160

Table (3) Tensile test results for single pass welding of AA 2024-T3

Tool rotational speed (rpm)	Welding travel speed (mm/min)	Average Yield strength 0.2% offset (MPa)	Ultimate tensile strength (MPa)	Elongation %	Weld efficiency %
Base metal		350	480	19.87	
370	24	237	343	3.43	72
	42	213	263	1.15	55
	74	198	215	0.68	45
475	24	230	300	1.52	62
	42	235	319	2.08	66
	74	188	212	0.61	44
650	24	220	279	1.29	58
	42	197	236	0.59	49
	74	185	208	0.46	43
820	24	215	239	0.64	50
	42	155	198	0.56	41
	74	156	156	0.32	32

Table (4) The tensile test results for double pass welding process (FSW and FSP)

First pass(FSW)		Second pass(FSP)		Average Yield strength 0.2% offset (MPa)	Ultimate tensile strength (MPa)	Elongation %	Weld efficiency %	Maximum Tensile Strength for Single Pass(MPa)	Reduction in Weld efficiency %
Welding direction	Tool revolution	Welding direction	Tool revolution						
Forward	c.w.	Forward	c.c.w.	210	332	4.84	69	343	3
Forward	c.w.	Forward	c.w.	212	275	1.37	57		15
Forward	c.w.	Backward	c.w.	216	313	2.31	65		7
Forward	c.w.	Backward	c.c.w.	203	294	2	61		11

Figures

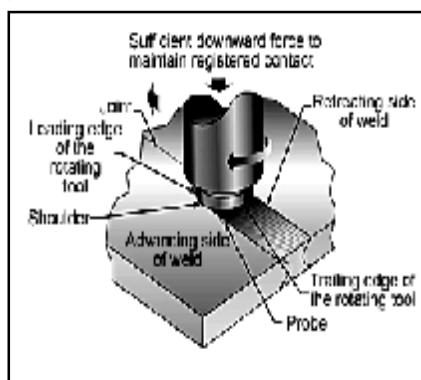


Figure (1) the schematic diagram of FSW.

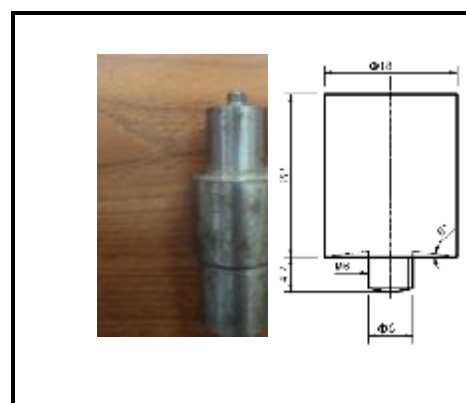


Figure (2) the configuration of the tool used.

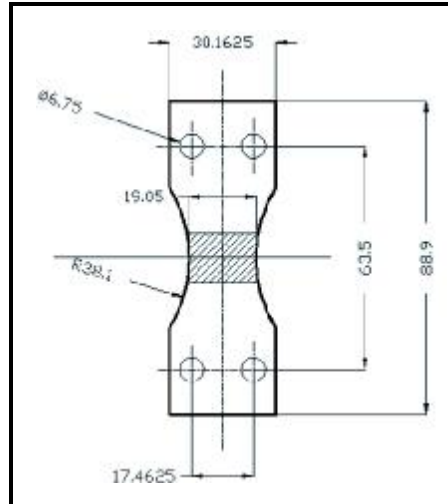


Figure (3) Fatigue specimen (DIN 50113)



Figure (4) Fracture surfaces showing theseparatingareabetween
Stir zone and the base metal



Figure (5) sudden fracture due to a (all dimensions in mm).
Wormhole defect

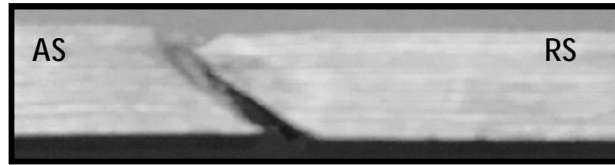


Figure (6) FSW joints failed at heat affected zone (HAZ) of the advancing side (AS)

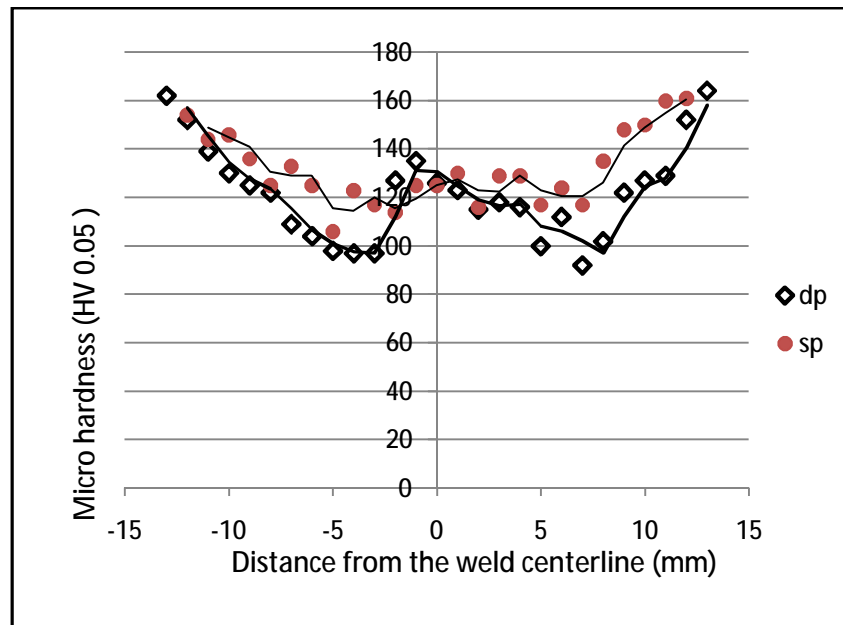


Figure (7) Hardness distribution across FSW joint at 370 rpm tool rotational speed and 24 mm/min welding travel speed for both single and double pass welded joints

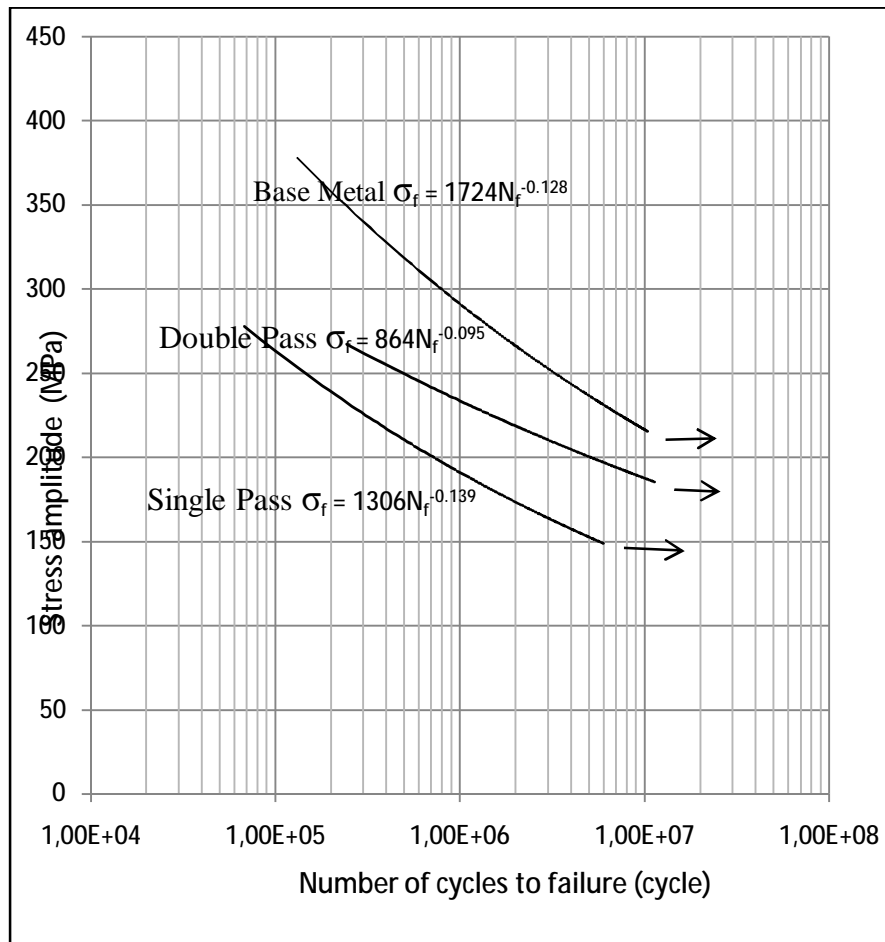


Figure (8) The S-N curves for the base metal, single pass (FSW), and doublepass (FSW and FSP) welded joints